

The ultraviolet spectrum of the peculiar post-AGB star HD 101584

Eric J. Bakker

SRON Laboratory for Space Research
Sorbonnelaan 2
NL-3584 CA Utrecht
The Netherlands

received March 12 1993, accepted june 13 1993

Abstract. The high-resolution ($R \approx 10^4$) near-ultraviolet IUE spectrum of the peculiar post Asymptotic Giant Branch (post-AGB) supergiant HD 101584 (F0Iape) has been analyzed. In the wavelength range between 2500 and 3000 Å, 291 out of 332 absorption features are identified. The main contribution comes from FeII, CrII and MnII. Most of the absorption features are blends from several absorption lines. This is mainly due to the intrinsic broad line profiles in the spectrum of HD 101584 in combination with the many absorption lines which occur in the UV for a F-type spectrum.

The list compiled gives for all measured absorption features between 2500 and 3000 Å the measured central wavelength of the core of the profile, the equivalent width of the profile if this could be determined, the depth of the profile, an asymmetry factor, a quality factor and lists the transitions which are responsible for the feature. An analysis of the radial velocities of the absorption profiles will be give in a separate paper.

Key words: near-ultraviolet spectrum – spectral line identification

1. Introduction

The peculiar supergiant HD 101584 has been classified as a F0Iape star (Hoffleit *et al.* 1983). The star is associated with a strong infrared source (Humphreys & Ney 1974a 1974b; Parthasarathy & Pottasch 1986), which is normally interpreted as a combination of cold and hot dust. HD 101584 does also show several millimeter CO($J = 1 \rightarrow 0$) emission features (Trams *et al.* 1990; Loup *et al.* 1990) and outwards accelerated bipolar OH maser emission (Te Lintel Hekkert *et al.* 1992). Radial velocity measurements

of absorption lines show variations which are not well understood yet. It is not evident that these variations are due to binarity of the system.

Table 1. Data on HD 101584 and α Lep

	HD 101584	HD 36673
	α Lep	
$\alpha[2000]$	11 ^h 40 ^m 58.8 ^s	05 ^h 32 ^m 43.7 ^s
$\delta[2000]$	-55° 34' 25"	-17° 49' 20"
b^{II}	+5.94°	-25.14°
l^{II}	293.03°	220.95°
Spectral Type	F0Iape	F0Ib
App. Visual Magn.	7.01	2.58
$B - V$	0.39	0.21
$v \sin i$ [km s ⁻¹]		15

Information based on Hoffleit (1983)

Humphreys (1976) suggested that the object is a binary system with a period of 3.5 years. In this model the strong IR excess is attributed to a secondary cool M-type star which fills its Roche lobe. The primary, the observed star, is a hot accreting A (or B) star which accretes gas and dust form the secondaries Roche lobe. The A-type star is thus observed with a F-type like spectrum. The mass-loss from the secondary produces a common envelope around the system which give a P-Cygni profile of e.g. the H α line.

An alternative model for this object is by Parthasarathy and Pottasch (1986). They suggest that HD 101584 is a transition object form the AGB to the planetary nebula stage, the post Asymptotic Giant Branch (post-AGB) phase. The large infrared excess can be explained by the combination of a hot and a cold dust shell of 750 and 120 K respectively. A study by

Trams *et al.* (1991) classifies HD 101584 as a post-AGB star on basis of its infrared excess and galactic latitude.

An extension of the post-AGB theory has been made by Trams *et al.* (1990). They discuss the millimeter CO($J = 1 \rightarrow 0$) emission features of HD 101584 in terms of multiple ejections of shells, or the diametrical ejections of blobs. The CO peak at the stellar rest velocity, and the narrow stationary optical emission lines could originate from a flattened envelope (or disk).

The aim of this study is to investigate this interesting star in order to gain insight in the evolution of post-AGB binaries and to extend our current knowledge of HD 101584 from the radio, millimeter, infrared and optical to the ultraviolet by making a UV spectral line identification. The compiled list (Table 6) is an absorption line identification between 2500 Å and 3000 Å based on IUE spectra. This list will be subject to further study on the radial velocities of the identified lines and on the asymmetry of the line profiles measured.

The spectra used are obtained with the International Ultraviolet Explorer (IUE). The 1900 to 3200 Å UV band has been detected in high-resolution mode ($R \approx 10^4$), which gives a velocity resolution of approximately 6 km s⁻¹ (Kondo 1987). For wavelengths shortwards of 2500 Å the moderate interstellar and circumstellar extinction, in combination with the decrease of the continuum level, give a too low signal-to-noise ratio to make a reliable identification possible. For wavelengths longwards of 3000 Å the echelle orders do not fully overlap and this introduces blind spots in the spectrum. For these two reasons this study limits itself to the line identification in the spectral range between 2500 and 3000 Å. By comparing the spectrum of HD 101584 with a standard F-type supergiant α Lep (F0 Ib), a line identification is made on basis of a multiplet fit technique as described in Sect. 3.1. By a first comparison of the spectrum of HD 101584 with the comparison star α Lep it is evident that the absorption features in HD 101584 are intrinsically broader than the corresponding features in α Lep (Fig. 1). This effect accounts for the numerous strongly blended features and a poorly defined continuum level of the spectrum.

The result of this study is a list (Table 6) of 332 absorption features of the object HD 101584 in the wavelength region between 2500 and 3000 Å. We also provide information on the observed central wavelength, equivalent width, depth of the feature with respect to the adopted local continuum, an asymmetry factor, and the possible contribution of various blends to the absorption features. The data for the absorption lines are from Moore's (1950 and 1962) ultraviolet multiplet tables.

2. The observations

The observations discussed in this paper are high-resolution long wavelength spectra, LWP17369, LWR4052 and LWR5781 made with the International Ultraviolet Ex-

plorer (IUE) as described in Kondo (1987). The observational parameters of the spectra are given in Table 1 and 2 and the raw IUE image were processed with the Starlink program IUEDR (version 1.3). The extracted spectra were used for this study. Due to the lack of clearly detectable interstellar absorption lines it was not possible to make an absolute wavelength calibration based on interstellar absorption lines. For LWP17369 we used the heliocentric velocity correction from the IUE software. For LWR5042 and LWR5781 no heliocentric velocity corrected were available from the IUE log file and we corrected for the earth motion and neglected the additional satellite velocity. This introduces a systematic velocity shift of one spectrum to another with a maximum velocity of 3.3 km s⁻¹. There was no attempt made to reprocess the reference spectrum of α Lep.

3. The line identification

3.1. The method

The high-resolution near-ultraviolet spectrum of the supergiant HD 101584 is characterized by intrinsically broad absorption lines (Fig. 1). This results in a spectrum containing numerous strongly blended absorption features and a not well determined continuum level. By comparison of the spectrum of HD 101584 with a standard F-type supergiant, α Lep (F0 Ib), the line identification is simplified. Since the IUE spectrum of HD 101584 has intrinsically broad absorption lines, it seems almost useless to try to make an identification by means of some kind of automatic computer algorithm. The spectral identification described in this work is therefore based on individual multiplet fitting. The identification is made for the IUE spectrum LWP 17369 with LWR 5042 to fill in the missing data points of the former spectrum. The missing data points are due to reseau marks and wavelength gaps between two successive echelles. The absorption features measured from this second spectrum are marked with an asterisk (*) in Table 6. The data of these features should not be mixed with the data of features from the other spectrum, because there seem to be absorption line dependent velocity and intensity variations.

From the literature (Van der Hucht *et al.* 1976) a first estimate about the multiplets which makes the largest contributions to the broad features could be obtained. Starting with the most conspicuous multiplets, FeII 60, 61, 62 and 63, all lines of a given multiplet were checked to see if there was a corresponding absorption feature in the spectrum near the laboratory wavelength for this line. A multiplet was designated "detected" if most of the multiplet lines were measured with an equivalent width ratio in agreement with the intensity values as given in the multiplet table and a consistent Doppler velocity of the lines within one multiplet. However due to the large number of blended lines in the spectrum, it was not always evident

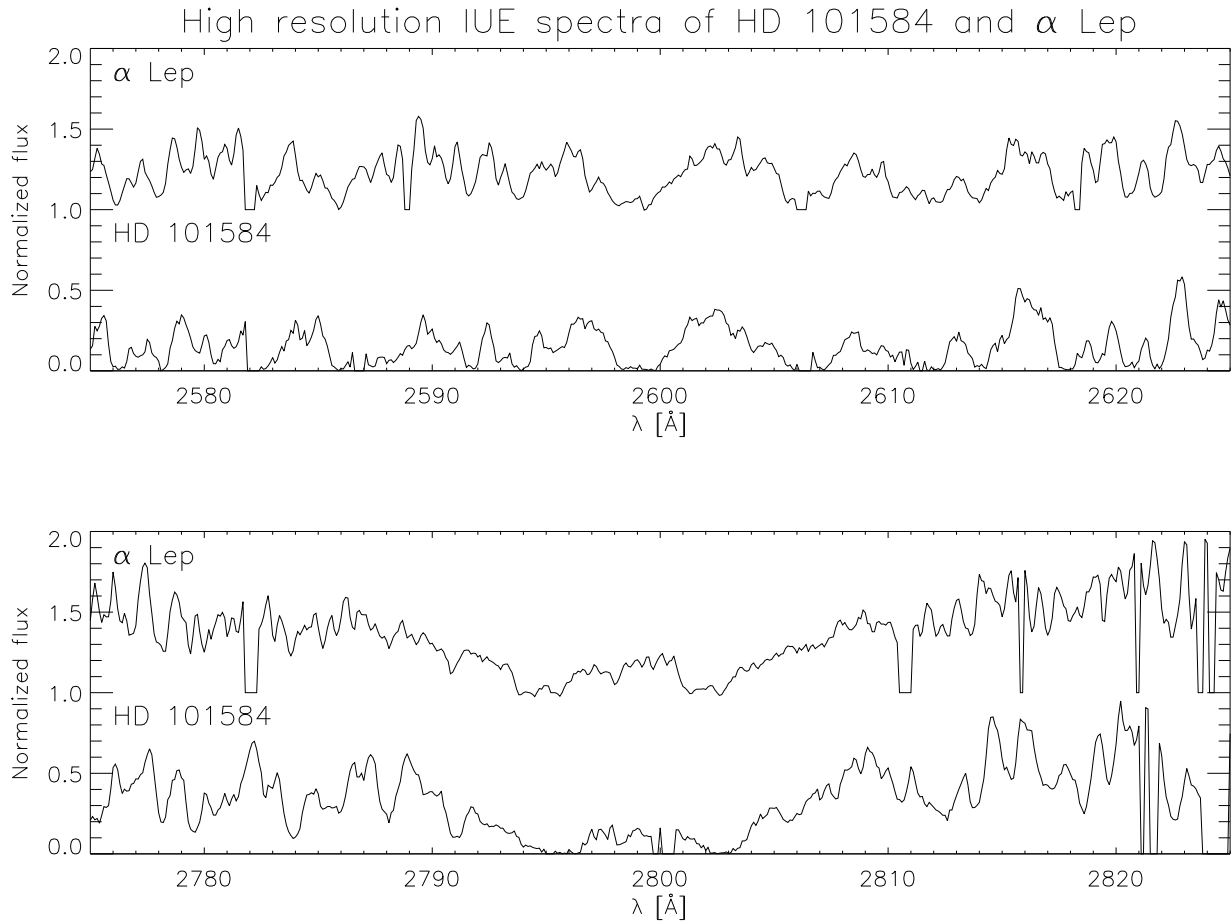


Fig. 1. The ultraviolet spectrum of the peculiar supergiant HD 101584 (LWP17369) and of the normal supergiant α Lep (LWR5781). The absorption lines in the spectrum of HD 101584 are intrinsically broader than the corresponding absorption lines in α Lep. The normalized flux of α Lep is shifted by +1 to allow a better comparison with HD 101584. The spectra are not heliocentrically corrected in this plot

that a multiplet was detected and the decision was based on common sense.

The multiplet fitting technique was finished when most of the absorption features were identified. The remaining features were identified by looking up the apparent central wavelength of the absorption feature in the finding list. Possible candidate lines were selected on basis of a multiplet fit. Some features remained unidentified. By looking up these features in the Moore *et al.* (1982) solar spectrum atlas, some of them could be identified.

This method of line identification makes use of only a limited number of multiplets. Using the foreknowledge of previous line identifications on F-type supergiant spectra, one limits oneself by checking only the multiplets which have a high chance of being detected. This means that low abundance elements are not checked, nor higher ionization degrees than expected for a F-type spectrum, nor those multiplet which have a high excitation level. The disadvantage of this technique, that only the expected ions

will be tested, and that anomalies are not recognized, is lifted by introducing a comparison star. The spectrum of HD 101584 only shows small differences with the reference spectrum of α Lep. The most prominent difference is the intrinsic broad lines profiles in the spectrum, but there seems to be no significant different abundance pattern, nor additional lines.

The final absorption feature line-identification list of the ultraviolet spectrum (2500–3000 Å) of HD 101584 is given in Table 6. It lists the main characteristics of the features, possible candidate absorption lines, and gives the actual identification made in this study. The heliocentric velocities derived from the apparent central wavelength of the feature and the laboratory wavelength are also given.

3.2. Description of the tables

The format of the table is as follow:

Table 2. Information on the spectra of HD 101584

	HD 101584	HD 101584	α Lep
Image	LWP17369	LWR5042	LWR5781
Observation date	15 Febr. 1990	14 July 1979	10 Aug. 1979
Aperture	large	large	small
Integration time	140 minutes	120 minutes	10 minutes
Ground Station	Vilspa (Spain)	Goddard	Goddard
Reprocessed	IUEDR 1.3	IUEDR 1.3	10 Aug. 1979
Heliocentric corrected	Yes	Yes	Yes

1. $\lambda_{\text{obs.}}$ [\AA]: the observed central wavelength of the absorption feature
2. W [\AA]: the observed equivalent width. The error on the given equivalent width is about 25% which is mainly due to the lack of a well defined continuum level. If one of the wings of the profile could not be measured, the equivalent width is calculated assuming a symmetric profile. If both wings could not be measured this space is left blank
3. D [%]: the depth of the profile with respect to the adopted local continuum. This value ranges from 100, very strong absorption, to almost 0, for very weak absorption
4. A : the asymmetry factor defined as the ratio of the red over blue equivalent width. A symmetric profile has an asymmetry factor of one. For features which have an excess of red absorption, the asymmetry factor is greater than one. For features with extra blue absorption the asymmetry factor is smaller than one. If one of the wings could not be measured a code is given: a “R B” (red blended) or “B B” (blue blended) for the lack of a measurement of the red or blue wing respectively
5. Q : the quality factor for the identification and the absorption feature. If the quality factor is “3” the line is positively identified with one absorption line. Blends of this line are of minor importance. The lines marked with a “3” can be used for further study on the velocities and asymmetry of the line. A quality of “2” means that either the line is weakly blended, or the same absorption feature in α Lep is split into two components, or there is more than one good candidate absorption line. A quality of “1” is an unreliable line for further study. The identification made is however correct, but there are strong blends, or the line is very weak. If the quality factor is followed by an asterisk the data of the absorption feature is from the additional spectrum (LWR5042)
6. $\lambda_{\text{lab.}}$ [\AA]: the laboratory wavelength of the candidate line
7. ion(mult): the element and multiplet number for the given absorption line
8. χ [eV]: lower level excitation energy of transition which give the candidate absorption line
9. C : contribution of the blends to the observed line. A candidate absorption line marked with a “P” is the **primary contributor** to the feature. “S” the secondary, and “M” for lines which give only a minor contribution to the features.
10. v [km s^{-1}]: radial heliocentric velocity for identified absorption feature
11. remarks: remarks on the line identification. “U” stands for unidentified feature

4. Discussion

In the wavelength range between 2500 and 3000 \AA , 332 absorption features have been measured and tabulated in Table 6. 291 of the features could be identified. Most of them have only one primary contributor. An overview of all transitions which are marked as primary contributor is given in Table 3. As expected the spectrum is strongly dominated by FeII, which is the main degree of ionization of Fe in the spectrum of HD 101584. It seems that there are also some lines from SiII and TiII in the spectrum.

Table 3. An overview of the ions marked as principal contributor to an absorption feature in the UV spectrum of HD 101584. Of the 332 features, six have two primary contributors, the others only one. The number of occurrences as primary contributor in the identification list

Ion	No.	Ion	No.
Unidentified	41		
Mg I	8	Cr I	1
MgII	7	CrII	62
Si I	4	MnII	47
TiII	4	Fe I	12
V II	19	FeII	133

The 41 unidentified features are tabulated in Table 4. For seven of these features a possible identification could be made as given in Table 5.

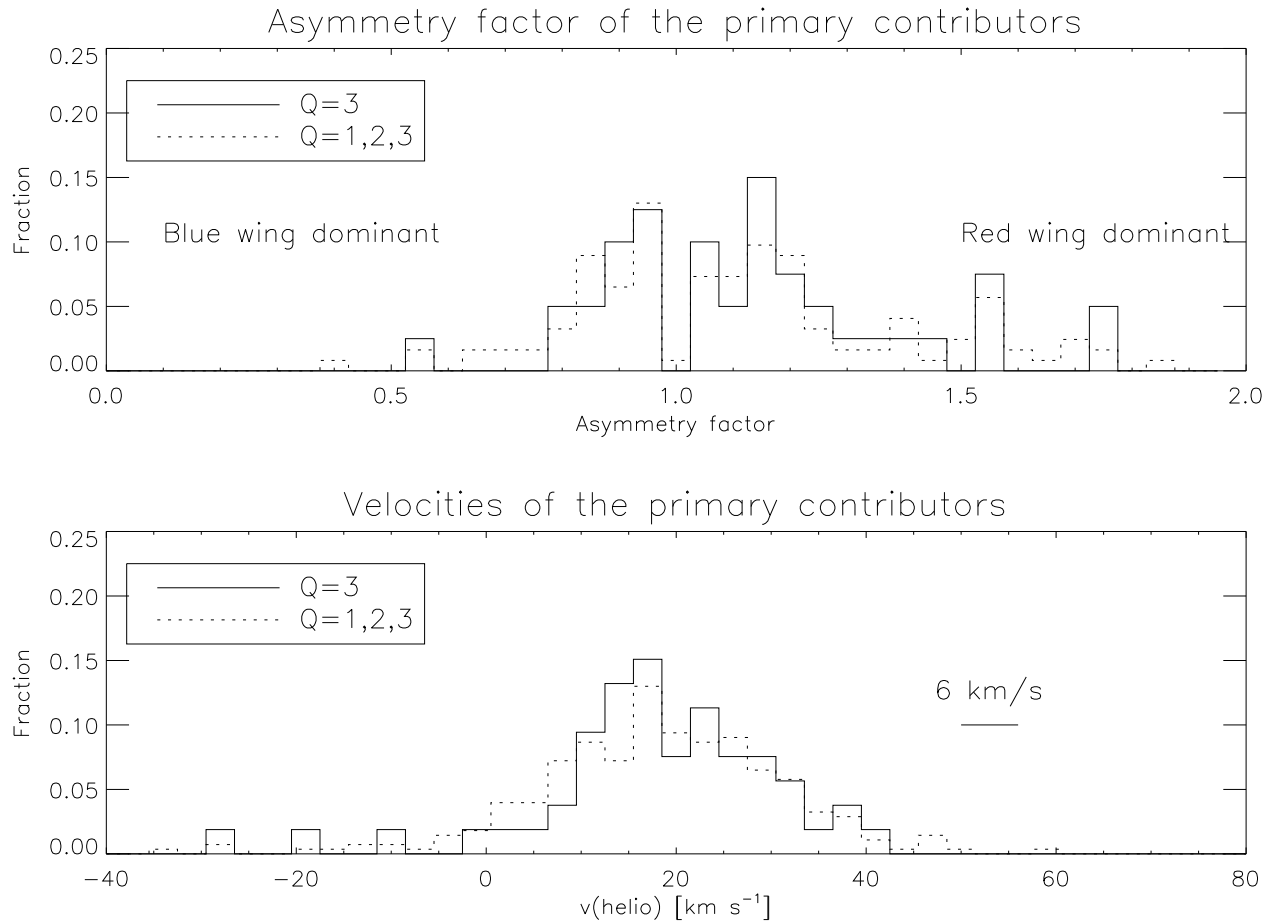


Fig. 2. The upper histogram shows a numbercount on the asymmetry factor. It is noted that the factor does not spread around 1 but rather on a value a little bit higher. The lower histogram is a numbercount on the velocities. The IUE resolution predicts an accuracy of 6 km s^{-1} , significant smaller than measured in this spectrum. The histograms are made for all transitions marked with a “P” and all quality factors (dashed line). The solid lines are made by using only the quality $Q = 3$ lines. The histograms are normalized on 1 to allow comparison

Table 4. Unidentified features in the spectrum of HD 101584

$\lambda_{\text{obs}} [\text{\AA}]$				
2508.14	2616.00	2705.05	2807.06	2901.52
2508.69	2637.00	2716.25	2808.81	2904.42
2522.09	2641.50	2735.16	2818.56	2966.37
2552.44	2642.35	2737.26	2819.76	2968.57
2553.89	2649.75	2770.86	2820.81	2983.67
2557.49	2655.25	2773.06	2833.76	
2584.49	2683.10		2834.61	
2587.34	2686.25		2836.56	
2589.09			2839.26	
2592.84			2845.71	
			2884.22	
			2888.30	

Table 5. Possible identification of unidentified features

$\lambda_{\text{obs}} [\text{\AA}]$	Poss. ident.
2589.09	MnII
2616.00	Fe I
2683.10	V II (I.S.)
2735.16	ZrII
2820.81	OH
2834.61	Fe I
2983.67	NiII

Table 6 gives the opportunity to look at the statistics on the velocities and on the asymmetry factor.

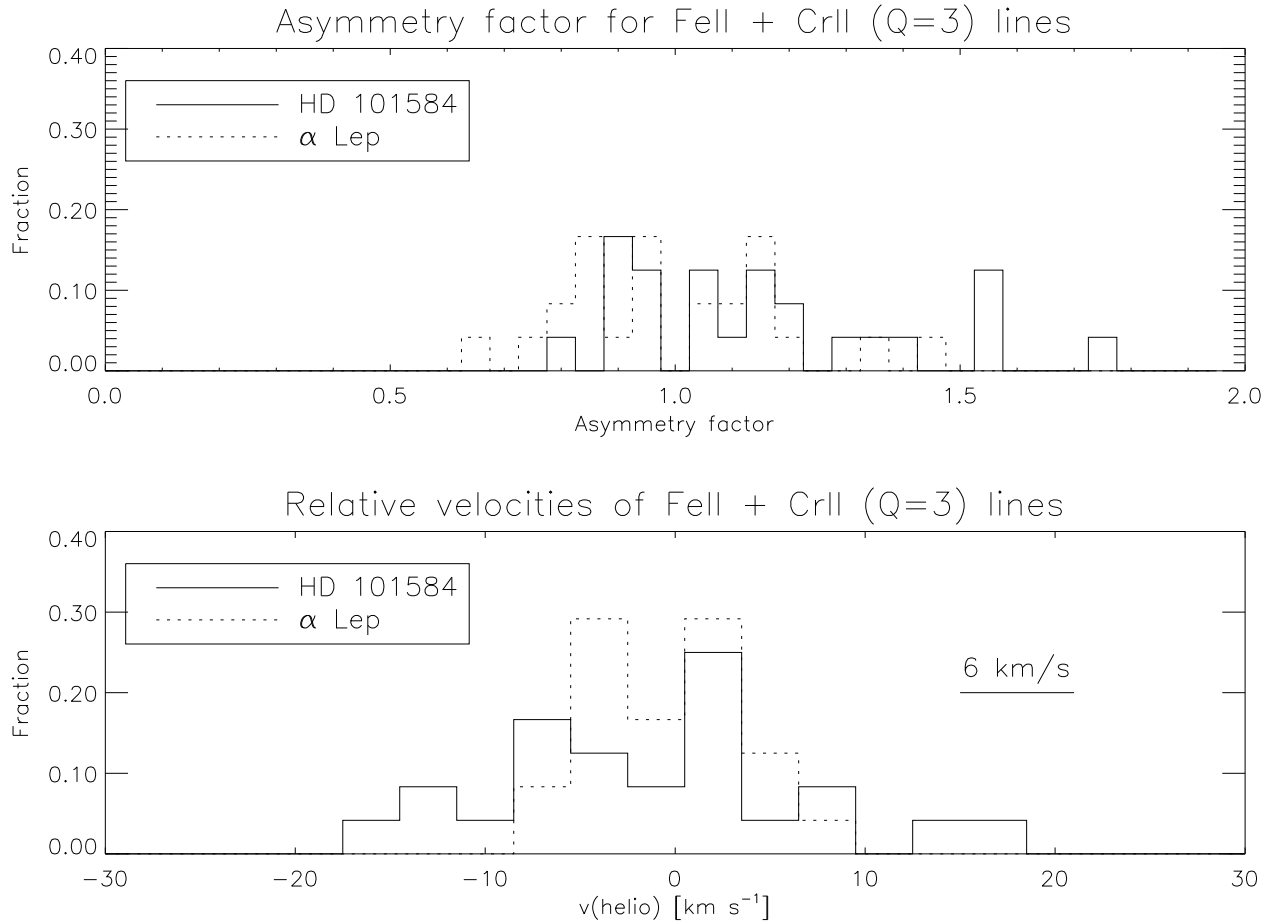


Fig. 3. The upper histogram shows a numbercount on the asymmetry factor, the lower on the velocities relative to the average velocity. In this figure only the FeII and CrII lines with a quality factor of $Q = 3$ are used and which occur in the spectra of both stars. It is noted that the asymmetry factor for HD 101584 is on the average larger than for α Lep, and that the asymmetry factor for HD 101584 is not centered around 1. The velocity spread in α Lep is as expected from the IUE resolution. The spread on the same lines in HD 101584 is significant larger than expected.

4.1. Asymmetric line profiles

Fig. 2 shows the number of profiles within a given range of asymmetry factors. There is a tendency for an asymmetry factor larger than one. This means that the slope of the red wing of the profile is less steep than the blue wing. This is unexpected because for photospheric lines one expects unity, and for wind line a value smaller than one.

By making a comparison of HD 101584 with α Lep using only those lines which have a high quality (FeII and CrII with $Q = 3$) it is clear that the asymmetry factor in HD 101584 is larger than for α Lep (Fig. 3).

4.2. Large velocity spread in measured Doppler velocities

From Kondo 1987 a velocity spread from $\pm 6 \text{ km s}^{-1}$ based on the IUE resolution is expected, it is however clear from Fig. 2 that the real spread in measured Doppler velocities is much larger for the lines which are marked as primary

contributor to an absorption feature. A study on this interesting problem is in progress. (Bakker 1993).

By making a comparison of HD 101584 with α Lep using only those lines which have a high quality (FeII and CrII with $Q = 3$) it is clear that the velocity spread in HD 101584 is larger than for α Lep.

4.3. Curve of Growth for FeII

To see whether the quality factor has any significance, a curve of growth (COG) for the FeII identification with $Q = 3$ in α Lep has been made (Fig. 4). It is evident from the figure that the $Q = 3$ annotation is a strong one, although there are data points for α Lep which seem to have a too low equivalent width. The COG of the same identified line of FeII for HD 101584 is superimposed in this figure. The horizontal part of the COG for HD 101584 is significantly shifted up due to a broadening mechanism

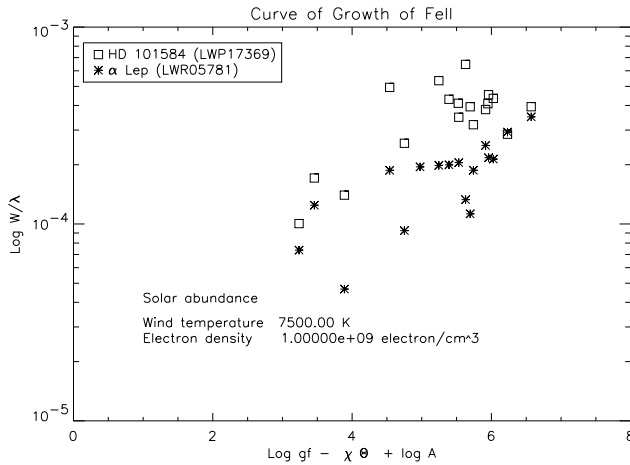


Fig. 4. The Curve of Growth for α Lep and HD 10158. Only the Fe II lines with a quality factor $Q = 3$ are used in this graph. The data points for HD 101584 are higher in comparison to α Lep. This shows the presence of an extreme broadening mechanism of the absorption profiles. The data points of α Lep seem to follow a standard COG curve, which imply that the $Q = 3$ annotation is a strong one

of the absorption features, whereas the spread in the data points is also larger than for the reference star.

Acknowledgements. The author wants to thank Henny Lamers, Rens Waters and Christoffel Waelkens for the many stimulating and constructive discussions on this work, Norman Trams for making the ultraviolet spectrum of HD 101584 available for this study. Lex Kaper is thanked for the help with the IUEDR data reduction package. The author was supported by grant no. 782-371-040 by ASTRON, which receives funds from the Netherlands Organization for the Advancement of Pure Research (NWO). This research has made use of the Simbad database, operated at CDS, Strasbourg, France.

References

- Bakker E.J., 1993: in Proceedings of International Workshop on Luminous High-Latitude stars, ASP Conference Series 45, Ed. D.D. Sasselov, page 130
- Hoffleit D., Saladiga M., Wlasuk P.: 1983, "Supplement to the bright star catalogue", Yale University Observatory, USA
- Humphreys R.M., Ney E.P.: 1974a, ApJ 187, L75
- Humphreys R.M., Ney E.P.: 1974b, ApJ 190, 339
- Humphreys R.M.: 1976, ApJ 206, 122
- Kondo Y. (eds.): 1987, "Exploring the Universe with the IUE satellite", Kluwer Academic Publishers, page 741
- Te Lintel Hekkert P., Chapman J.M., Zijlstra A.A.: 1992, ApJ 390, L23
- Loup C., Forveille T., Nyman L.Å. Omont A.: 1990, A&A, 227, L29
- Moore Ch.E.: 1950, "An Ultraviolet Multiplet Table", NBS Circ. no. 488, § 1
- Moore Ch.E.: 1962, "An Ultraviolet Multiplet Table", NBS Circ. no. 488, § 3
- Moore Ch.E., Tousey R., Brown C.M.: 1982, "The Solar Spectrum 3069 – 2095 Å"
- Parthasarathy M., Pottasch S.R.: 1986, A&A 154, L16
- Trams N.R., Van der Veen W.E.C.J., Waelkens C., Waters L.B.F.M., Lamers H.J.G.L.M.: 1990, A&A 233, 53
- Trams N.R., Waters L.B.F.M., Lamers H.J.G.L.M., Waelkens C., Geballe T.R., Thé P.S.: 1991, A&AS 87, 361
- Van de Hucht K.A., Lamers H.J.G.L.M., Faraggiana R., Hack M., Stalio R.: 1976, A&AS, 25, 65

Table 6. UV line identification of HD 101584 (2500 to 3000 Å)

λ_{obs} [Å]	W [Å]	D [%]	A	Q	λ_{lab} [Å]	ion(mult)	χ [eV]	C	v [km s $^{-1}$]	remark
2501.14	0.54	94		1	2500.919	FeII(357)	4.71	P	27	
2502.69		94		1	2502.388	FeII(207)	3.21	P	36	
2505.34	0.87	100	1.60	2	2505.217	FeII(033)	0.30	P	15	
2508.14		76		2				P		U
2508.69		73		2				P		U
2509.34	1.24	87	0.91	3	2509.117	FeII(242)	3.23	P	27	
2512.69	0.43	61	1.00	2	2512.513	FeII(343)	4.46	P	21	
					2512.727	FeII(129)	2.63	S		
2513.59		81		3	2513.372	FeII(207)	3.19	P	26	
2516.24	0.42	69	2.78	3	2516.109	Si I(001)	0.03	P	16	
2516.74		58		3	2516.597	MnII(021)	3.40	P	17	
2517.49		85		1	2517.211	FeII(207)	3.21	P	33	
					2519.044	FeII(268)	3.37	S		
2519.34		90		2	2519.203	Si I(001)	0.01	P	16	
2521.02		98		1*	2521.089	FeII(268)	3.41	P	-7	
2522.09		98		2				P		U
2522.34		92		1	2522.189	FeII(159)	2.62	P	18	
2524.29		71		2	2524.108	Si I(001)	0.01	P	22	
2526.49		95		1	2526.292	FeII(145)	2.57	P	24	
2527.39		100		1	2527.107	FeII(159)	2.65	P	34	
2528.59		84		1	2528.510	Si I(001)	0.03	P	9	
2529.19		87		1	2529.078	FeII(357)	4.72	P	13	
2529.64		100		1	2529.48	CrII(009)	1.50	P	19	
					2529.545	FeII(145)	2.69	M		
2531.34	1.10	98	1.24	2	2531.082	FeII(033)	0.35	P	31	
2532.04	0.95	84	1.14	1	2531.84	CrII(009)	1.52	P	24	
2533.79	1.15	100	R B	3	2533.626	FeII(159)	2.65	P	19	
2534.49		97		1	2534.413	FeII(159)	2.68	P	9	
2535.94		100		2	2535.657	MnII(021)	3.41	P	33	
2538.79		100		1	2538.577	FeII(268)	3.41	P	25	very weak
					2539.003	FeII(158)	2.62	S		
2540.04	0.99	85	1.11	2	2539.52	CrII(009)	1.52	P	61	high velocity
2540.79		97		1	2540.669	FeII(343)	4.48	P	14	
2541.24		98		2	2541.113	MnII(022)	3.41	P	15	
2541.99		97		1	2541.831	FeII(158)	2.68	P	19	
2543.09		94		1	2542.922	MnII(021)	3.41	P	20	
					2543.382	FeII(159)	2.66	S		
2543.69		95		1	2543.458	MnII(021)	3.41	P	27	
2545.29		94		1	2545.215	FeII(159)	2.68	P	9	
					2548.590	FeII(158)	2.66	S		
2548.79		98		1	2548.741	FeII(145)	2.69	P	6	
2550.84		97		2	2550.575	FeII(158)	2.65	P	31	
2551.84		74		1	2551.58	CrII(109)	3.85	P	31	
2552.44		89		2				P		U; α Lep double
2553.89	0.66	80	1.00	1				P		U; double
2556.09		81		1	2555.988	TiII(009)	0.57	P	12	
2556.79		81		1	2556.572	MnII(020)	3.41	P	26	

Table 6. continued

λ_{obs} [Å]	W [Å]	D [%]	A	Q	λ_{lab} [Å]	ion(mult)	χ [eV]	C	v [km s ⁻¹]	remark
					2556.893	MnII(020)	3.41	S		
2557.19		92		1	2557.079	FeII(158)	2.68	P	13	
2557.49		90		1				P		U
					2557.45	CrII(089)	3.74	M		
2558.69	0.56	81		2	2558.604	MnII(020)	3.40	P	10	
2559.64		95		1	2559.415	MnII(020)	3.41	P	26	
2559.79		95		1	2559.677	MnII(020)	3.41	P	13	
					2559.745	MnII(020)	3.41	S		
2562.19		87		1	2562.094	FeII(221)	3.18	P	11	
2562.74		100		1	2562.535	FeII(064)	0.98	P	24	
2563.69		100		2	2563.472	FeII(064)	1.04	P	26	
					2563.58	CrII(089)	3.75	S		
					2563.640	MnII(020)	3.40	M		
2563.99		94		1	2563.834	FeII(266)	3.41	P	18	very weak
2565.59	0.35	69	1.22	3	2565.219	MnII(020)	3.40	P	43	
2566.14		40		1	2566.034	MnII(020)	3.41	P	12	
2566.59		85		1	2566.52	CrII(089)	3.73	P	8	
2567.04	1.20	98	0.92	2	2566.908	FeII(064)	1.07	P	15	
2570.09	0.44	74	0.82	3	2569.775	FeII(266)	3.41	P	37	
2571.24	0.80	90	R B	2	2571.036	TiII(009)	0.60	P	24	
2573.24	1.20	82	R B	1	2572.965	FeII(190)	2.88	P	32	too strong
2573.89		76		1	2573.72	TiII(009)	0.60	P	20	
					2574.18	CrII(089)	3.72	M		
2574.49	1.30	97	1.43	1	2574.363	FeII(144)	2.57	P	15	
2576.24	1.20	97	1.71	2	2576.107	MnII(001)	0.00	P	15	
2578.09	1.30	98	1.00	1	2577.920	FeII(064)	1.09	P	20	variable
					2578.31	CrII(089)	3.73	M		
2579.69		77		1	2579.406	FeII(266)	3.41	P	33	
2581.29	0.56	73	0.86	2	2581.111	FeII(190)	2.88	P	21	
2583.49		74		1	2583.343	FeII(266)	3.37	P	17	
2584.19		60		2	2584.10	CrII(089)	3.72	P	10	
2584.49		68		1				P		U
2585.94	1.57	100	R B	1	2585.876	FeII(001)	0.00	P	7	
2587.34		95		3				P		U
2588.29		89		2	2588.182	FeII(145)	2.77	P	13	
					2588.25	CrII(089)	3.73	M		
					2588.786	FeII(265)	3.37	M		
2589.09		73		2				P		U; MnII in Sun
2590.79		81		1	2590.548	FeII(145)	2.69	P	28	too strong
					2591.432	MnII(036)	3.69	S		
2591.74	1.49	98	1.00	2	2591.542	FeII(064)	1.04	P	23	double peaked
2592.84		89		2				P		U
2593.89	1.64	98	0.90	2	2593.722	FeII(064)	1.09	P	19	double peaked
					2593.731	MnII(001)	0.00	M		
2595.07		82		1*	2595.285	FeII(172)	2.79	P	-24	
2599.09	3.30	100	1.23	1	2599.395	FeII(001)	0.00	P	-34	
2601.75		47		1	2601.521	MnII(054)	4.05	P	26	
					2601.58	CrII(088)	3.72	S		

Table 6. continued

λ_{obs} [Å]	W [Å]	D [%]	A	Q	λ_{lab} [Å]	ion(mult)	χ [eV]	C	v [km s $^{-1}$]	remark
2604.15		79		2	2603.721 2605.416	MnII(036) FeII(204)	3.69 3.22	P S	49	too strong
2605.75		100		1	2605.697 2607.06	MnII(001) CrII(087)	0.00 3.75	P M	6	
2607.15		100		1	2607.086 2608.80	FeII(001) CrII(087)	0.08 3.72	P M	7	
2609.00		79		1	2608.852	FeII(171)	2.79	P	17	
2610.30		90		1	2610.202	MnII(019)	3.40	P	11	
2612.05		100		1	2611.873 2613.576	FeII(001) FeII(172)	0.05 2.79	P	20	
2614.00	1.76	100	0.81	2	2613.820 2614.867	FeII(001) FeII(171)	0.11 2.82	P	21 27	double peaked
2615.10		71		1	2615.729	FeII(297)	3.87	M		
2616.00		24		1				P		U; Fe I in Sun
2616.60		40		1	2616.506 2616.506	MnII(019) MnII(019)	3.40 3.40	P	11	
2617.81	1.50	100	1.15	1	2617.618 2618.142	FeII(001) MnII(019)	0.09 3.40	P	22	
2618.40		85		1	2618.142	MnII(019)	3.40	P	30	
2619.20	1.40	92	0.95	3	2619.071	FeII(171)	2.79	P	15	double peaked
2620.45	1.20	97	R B	1	2620.175 2620.408	FeII(173) FeII(001)	2.83 0.11	P	31	
2620.80		97		1	2620.693 2620.693	FeII(171) FeII(171)	2.82 2.82	P	12	
2621.80	1.05	98	1.12	2	2621.669	FeII(001)	0.12	P	15	double peaked
2623.80	0.95	89	1.00	2	2623.721 2625.606	FeII(171) MnII(019)	2.83 3.41	P	9	
2625.70	1.67	100	R B	1	2625.664 2626.499	FeII(001) FeII(173)	0.05 2.84	P	4	
2628.45	1.38	100	0.56	1	2628.291 2628.569	FeII(001) FeII(203)	0.12 3.22	P	18	
2629.90		95		1	2629.590	FeII(171)	2.83	P	35	
2630.20		90		1	2630.068 2630.93	FeII(171) CrII(063)	2.84 3.74	P	15	
					2631.045	FeII(171)	2.82	S		
2630.81		100		3*	2631.045	FeII(001)	0.11	P	-26	
2631.31		97		1*	2631.321	FeII(001)	0.08	P	0	
2632.20		89		1	2632.011	MnII(019)	3.41	P	22	
2632.50		89		2	2632.353	MnII(019)	3.41	P	17	
2633.06	0.76	77	B B	3*	2633.200	FeII(356)	4.71	P	-15	
2635.60	0.54	69	1.00	1	2635.401 2636.46	FeII(238) CrII(062)	3.25 3.70	P	23	
					2636.687	FeII(356)	4.72	M		
2637.00	0.26	48	1.09	3	2637.643	FeII(221)	3.32	M		U
					2638.127	MnII(019)	3.41	M		
2638.20	1.56	89	1.25	1	2638.173	MnII(019)	3.41	P	3	blended

Table 6. continued

λ_{obs} [Å]	W [Å]	D [%]	A	Q	λ_{lab} [Å]	ion(mult)	χ [eV]	C	v [km s ⁻¹]	remark	
2639.90	0.70	77		1.00	1	2639.560 2639.850 2641.124	FeII(221) MnII(052) FeII(144)	3.32 4.05 2.69	P M M	39	double peaked
2641.50	0.35	65		1.22	3	2642.015	FeII(309)	3.93	M	U	
2642.35	0.56	76		0.63	3	2645.084	FeII(309)	3.93	S	U	
2645.40	0.32	68			2	2645.084	FeII(263)	3.37	P	36	
2648.10	0.22	40	R B	2		2648.08 2648.159	CrII(142) FeII(355)	3.99 4.71	P S	2	
2649.75	0.26	44		1.33	1				P	U	
2652.85	0.58	73		1.16	3	2652.496 2652.557	MnII(053) FeII(237)	4.06 3.25	P S	40	
2653.80	0.76	90		1.08	3	2653.57	CrII(008)	1.49	P	26	
2655.25	0.08	31		1.00	3				P	U	
2656.20	0.56	74		0.93	2	2655.920 2656.173 2658.251	MnII(052) MnII(070) FeII(309)	4.06 4.48 3.95	P M S	32	
2658.70	1.55	95		1.23	1	2658.59 2659.054	CrII(008) FeII(237)	1.48 3.25	P M	12	asymmetric
2660.91		48			1*	2660.755	MgII(004)	8.83	P	17	
2660.91		48			1*	2660.821	MgII(004) CrII(062)	8.83 3.74	P M	10	
2661.90	0.85	89		1.25	3	2661.73 2662.15 2662.541 2663.42	CrII(008) CrII(062) MnII(070) CrII(008)	1.50 3.74 4.49 1.52	P M M S	19	
2663.70	1.52	97		1.23	1	2663.67 2664.209	CrII(008) FeII(237)	1.48 3.25	P M	3	double peaked
2664.75	1.05	94		1.00	3	2664.665	FeII(263)	3.37	P	10	
2666.25	1.26	97	R B	1		2666.02 2666.631	CrII(008) FeII(263)	1.50 3.41	P M	26	
2666.90		90			1	2666.631	FeII(263)	3.41	P	30	
2669.00	1.20	94		1.22	1	2668.71 2670.06	CrII(008) CrII(063)	1.49 3.81	P S	33	
2670.45	0.68	76		0.89	2	2670.24 2670.384 2671.02 2672.310	CrII(069) FeII(355) CrII(061) FeII(202)	3.72 4.71 3.70 3.22	P S M M	24	
2673.10	1.25	94		0.80	1	2672.83	MnII(034)	3.69	M		
2677.45	1.07	92	R B	1		2677.13	CrII(008)	1.52	P	30	
2677.45	1.07	92	R B	1		2677.19 2677.851	CrII(008) MnII(052)	1.54 4.05	P M	29	
2678.10		73			1	2677.851	MnII(052)	4.05	P	28	
2679.10	1.58	97		0.91	1	2678.79 2679.165	CrII(007) MnII(052)	1.49 4.05	P M	35	

Table 6. continued

λ_{obs} [Å]	W [Å]	D [%]	A	Q	λ_{lab} [Å]	ion(mult)	χ [eV]	C	v [km s $^{-1}$]	remark	
2683.10	0.95	89		1.18	2			P		U; V II IS line ?	
2685.10	1.02	84	B B	1	2684.940	FeII(201)	3.14	P	18	too strong	
					2685.19	CrII(085)	3.72	M			
					2685.19	CrII(085)	3.73	M			
2686.25		76			1			P		U	
					2686.100	FeII(202)	3.22	M			
2687.30	1.10	94		1.10	3	2687.09	CrII(007)	1.50	P	23	very broad
					2687.60	CrII(084)	3.72	M			
2689.20		90			3	2689.03	CrII(084)	3.72	P	19	
2690.30		92			1	2690.067	Fe I(004)	0.00	P	26	
					2691.03	CrII(085)	3.74	S			
2691.15	1.38	95			2	2691.03	CrII(008)	1.54	P	13	
2691.85		71			1	2691.732	FeII(202)	3.19	P	13	
2695.65	0.41	68	B B		2	2695.363	MnII(034)	3.69	P	32	
2696.21		10			2*	2696.10	CrII(061)	3.74	P	12	
2698.00		82			1	2697.90	CrII(084)	3.74	P	11	
					2698.40	CrII(007)	1.52	M			
2698.70	1.80	98		0.76	1	2698.68	CrII(007)	1.48	P	2	
					2698.984	MnII(035)	3.69	M			
2701.10	0.54	83	R B		2	2700.944	V II(001)	0.04	P	17	
					2701.035	MnII(034)	3.69	M			
					2701.535	V II(002)	0.00	M			
					2701.65	CrII(062)	3.81	S			
2701.70		90			1	2701.693	MnII(018)	3.40	P	1	
2702.15	0.85	90			1	2701.990	Cr I(018)	1.03	P	18	
					2703.977	MnII(018)	3.40	M			
2704.20	1.05	92		1.18	2	2703.988	FeII(261)	3.37	P	24	
								P		U	
2705.05	0.62	52			2						
2706.20	1.10	94	R B	1	2705.727	MnII(018)	3.40	P	52		
					2706.17	V II(001)	0.03	S			
2707.70		81			2	2707.542	MnII(018)	3.40	P	18	
2708.05		74			1	2707.86	V II(002)	0.00	P	21	
2708.50		84			2	2708.445	MnII(018)	3.41	P	6	
2709.05		90			1	2709.051	FeII(218)	3.18	P	0	
2710.50	1.26	87	1.36		2	2710.332	MnII(018)	3.41	P	19	
					2711.566	MnII(018)	3.41	S			
2711.85		92			1	2711.632	MnII(018)	3.41	P	24	
					2711.740	V II(002)	0.04	M			
					2714.205	V II(002)	0.03	M			
2714.55	1.07	98		1.36	3	2714.414	FeII(063)	0.98	P	15	
					2715.676	V II(001)	0.04	S			
2715.70		94			1	2715.676	V II(001)	0.01	P	3	
2716.25		92			2			P		U	
2716.25		92			2	2716.216	FeII(261)	3.41	P	4	
2716.70		89			2	2716.683	FeII(062)	0.98	P	2	
2717.15		79			1	2716.795	MnII(033)	3.69	P	39	

Table 6. continued

λ_{obs} [Å]	W [Å]	D [%]	A	Q	λ_{lab} [Å]	ion(mult)	χ [eV]	C	v [km s ⁻¹]	remark
					2717.51	CrII(007)	1.48	M		
					2717.525	MnII(033)	3.69	M		
2717.70	87		2		2717.533	FeII(032)	0.23	P	18	
2719.05	92		3		2719.027	Fe I(005)	0.00	P	3	not in α Lep; IS?
2719.90	79		1		2719.736	MnII(033)	3.69	P	18	
2721.00	77		3		2720.902	Fe I(005)	0.05	P	11	
					2722.095	MnII(033)	3.69	S		
2722.35	85		1		2722.095	MnII(033)	3.70	P	28	
					2722.095	MnII(033)	3.70	M		
2722.70	1.32	94	1.00	1	2722.74	CrII(007)	1.49	P	-3	
					2723.218	V II(001)	0.03	M		
					2723.577	Fe I(005)	0.09	M		
2723.70		77		1	2723.64	CrII(059)	3.74	P	7	
					2724.462	MnII(033)	3.70	M		
2725.05	1.21	95	B B	1	2724.879	FeII(062)	1.04	P	19	
					2727.382	FeII(200)	3.14	M		
2727.70	1.44	97	1.60	2	2727.538	FeII(063)	1.04	P	18	
					2728.644	V II(001)	0.00	M		B
2728.95		81		1	2728.973	Fe I(004)	0.11	P	-2	variable
2730.90	0.78	95	1.00	3	2730.735	FeII(062)	1.07	P	18	
					2732.004	FeII(236)	3.25	M		
					2732.009	Mg I(009)	2.70	M		
2732.60	1.09	92	1.00	2	2732.441	FeII(032)	0.23	P	17	
					2733.509	Mg I(009)	2.70	M		
2734.01	0.24	40	1.00	3	2733.906	V II(001)	0.01	P	11	
					2734.07	CrII(060)	3.74	M		
2735.16		32		2	2736.500			P		U; Zr II
					2736.559	FeII(220)	3.32	M		
					2736.73	Mg I(009)	2.70	M		
					2736.73	CrII(061)	3.81	M		
2737.26	1.32	100	1.75	2	2737.19	CrII(061)	3.81	M		
					2737.310	Fe I(005)	0.11	M		
2739.91	1.52	100	1.21	2	2739.545	FeII(063)	0.98	P	40	variable
					2739.715	V II(001)	0.00	M		
					2740.09	CrII(006)	1.50	M		
					2741.563	V II(001)	0.03	M		
					2742.017	Fe I(004)	0.09	S		
2742.26	1.30	94	1.04	1	2742.02	CrII(006)	1.49	P	26	
					2742.43	V II(001)	0.00	M		
					2742.670	V II(013)	0.39	M		
2743.31	1.40	100	R B	1	2743.196	FeII(062)	1.09	P	12	
					2743.63	CrII(006)	1.48	M		
2745.26		65		3	2744.97	CrII(058)	3.74	P	32	
					2746.21	CrII(058)	3.70	M		
2746.81	1.85	100	1.33	2	2746.487	FeII(062)	1.07	P	35	
					2746.978	FeII(063)	1.04	M		

Table 6. continued

λ_{obs} [Å]	W [Å]	D [%]	A	Q	λ_{lab} [Å]	ion(mult)	χ [eV]	C	v [km s $^{-1}$]	remark
					2748.98	CrII(006)	1.49	M		
					2749.178	FeII(063)	1.07	S		
2749.46	2.08	100	1.90	2	2749.324	FeII(062)	1.04	P	15	
					2749.482	FeII(063)	1.09	M		
					2750.003	FeII(199)	3.19	M		
					2750.140	Fe I(005)	0.05	M		
2751.11		94		1	2750.72	CrII(006)	1.50	P	43	
					2750.896	FeII(200)	3.21	S		
2752.06	1.21	90	1.07	3	2751.85	CrII(006)	1.52	P	23	
2753.51	1.05	94	1.57	3	2753.289	FeII(235)	3.25	P	24	too strong
					2753.66	CrII(058)	3.70	M		
2755.81	1.32	98	1.42	2	2755.733	FeII(062)	0.98	P	8	
					2756.264	Fe I(004)	0.05	M		
					2756.329	Fe I(005)	0.11	M		
2756.66		85		1	2756.504	FeII(200)	3.22	P	17	
2757.96	1.10	86	0.68	2	2757.72	CrII(006)	1.50	P	26	variable
					2758.53	V II(013)	0.39	M		
2759.41	1.21	88	R B	2	2759.336	FeII(032)	0.30	P	8	double peaked
					2761.16	CrII(060)	3.81	M		
2762.01	1.20	95	R B	3	2761.813	FeII(063)	1.09	P	21	
2762.76	1.20	97	B B	2	2762.436	FeII(199)	3.22	P	35	
					2762.566	FeII(219)	3.18	S		
					2762.58	CrII(006)	1.52	M		
2764.11	0.85	74	1.57	1	2763.913	FeII(199)	3.21	P	21	
2764.81		74		1	2764.787	FeII(198)	3.14	P	2	
2765.91		74		2	2765.62	CrII(059)	3.81	P	31	
2766.66	1.40	94	0.92	3	2766.55	CrII(006)	1.54	P	12	
2767.76	1.13	85	1.00	3	2767.500	FeII(235)	3.23	P	28	
2769.11	1.08	98	1.75	2	2768.940	FeII(063)	1.07	P	18	double peaked
					2769.153	FeII(200)	3.21	M		
					2769.153	FeII(200)	3.21	M		
2769.51		97		2	2769.354	FeII(198)	3.14	P	17	
					2770.303	FeII(337)	4.46	M		
					2770.507	FeII(199)	3.21	M		
					2770.507	FeII(198)	3.14	M		
2770.86	0.62	69	1.00	1	2772.113	Fe I(005)	0.09	M		U
2773.06	0.84	70	1.14	2				P		U
2773.56		47		1	2773.30	CrII(058)	3.74	P	28	
2774.91		82		1	2774.686	FeII(218)	3.32	P	24	
					2776.180	FeII(199)	3.22	M		
2776.56	0.72	61	R B	1	2776.695	Mg I(006)	2.70	P	-14	
					2776.695	Mg I(007)	2.70	S		
					2777.892	FeII(233)	3.23	M		
					2778.221	Fe I(044)	0.86	M		
2778.11	0.89	79	1.50	3	2778.277	Mg I(006)	2.70	P	-17	weak
					2778.277	Mg I(007)	2.70	S		

Table 6. continued

λ_{obs} [Å]	W [Å]	D [%]	A	Q	λ_{lab} [Å]	ion(mult)	χ [eV]	C	v [km s $^{-1}$]	remark	
2779.56	1.13	87	1.17	3	2779.302 2779.832 2780.89 2781.418	FeII(234) Mg I(006) CrII(058) Mg I(007)	3.25 2.70 3.74 2.70	S P M S	-28	high velocity	
2781.31	1.12	69	B B	1	2781.418	Mg I(006)	2.70	P	-11		
2782.71	0.56	63	R B	1	2782.974	Mg I(006)	2.70	P	-27		
					2783.410	FeII(337)	4.46	M			
2783.91	1.80	90		1.18	3	2783.690	FeII(234)	3.23	P	24	
2785.26		71			1	2785.046	MnII(065)	4.29	P	23	
2788.01	0.41	79		1.67	2	2787.61 2790.752	CrII(058) FeII(032)	3.81 0.35	P S	43 poss Mg I	
2791.01	0.32	92		1.14	2	2790.768	MgII(003)	4.40	P	26	
						2795.167	MnII(066)	4.29	M		
2795.41	0.00	100	R B	1	2795.523	MgII(001)	0.00	P	-11		
					2797.914	FeII(234)	3.25	M			
2798.26		97			1	2797.989	MgII(003)	4.41	P	29	
2802.61	7.00	100	B B	1	2802.698	MgII(001)	0.00	P	-8		
					2805.207	MnII(051)	4.06	M			
2805.56		81			1	2805.359	MnII(066)	4.31	P	21	
2807.06		64			2			P		U	
2808.81		48			2			P		U; not in α Lep	
					2811.434	MnII(051)	4.06	M			
2811.71		69			1	2811.45	CrII(066)	3.72	P	28	
2812.16		81			1*	2812.258	MnII(071)	4.67	P	-9	
2813.81	0.75	73	0.88	2	2813.613 2814.22	FeII(198) CrII(083)	3.21 3.72	P M	21	too strong	
2815.31	0.50	53	0.75	2	2815.025	MnII(066)	4.32	P	30	not in α Lep	
2817.16		58			1	2816.83 2816.83 2817.838	CrII(058) CrII(081) TiII(025)	3.81 3.73 3.70	P S M	35	
					2818.08	CrII(067)	3.72	M			
2818.56	0.80	73	0.89	1				P		U	
					2818.66	CrII(067)	3.72	M			
					2819.327	FeII(196)	3.14	M			
2819.76	0.42	56	1.00	3				P		U	
2820.81	0.14	31	1.00	3				P		U; OH in Sun	
2822.56	1.00	79	1.16	1	2822.38 2822.668	CrII(082) FeII(231)	3.75 3.23	P S	19		
2823.31	0.72	73	0.67	3*	2823.276 2825.995	Fe I(044) Fe I(003)	0.95 0.09	P M	4		
2826.21	1.00	82	0.44	1	2826.024	FeII(255)	3.41	P	20		
2828.71		73			1	2828.622	FeII(231)	3.23	P	9	
					2830.08	CrII(083)	3.73	M			
2830.76	0.70	84	R B	3	2830.46 2830.60	CrII(082) CrII(081)	3.74 3.75	P M	32		
2832.61		77			1	2832.436	Fe I(044)	0.95	P	18	
2833.76	0.49	56	0.86	3				P		U	

Table 6. continued

λ_{obs} [Å]	W [Å]	D [%]	A	Q	λ_{lab} [Å]	ion(mult)	χ [eV]	C	v [km s ⁻¹]	remark
2834.61	0.52	56	1.20	2				P		U; Fe I
2835.91	1.32	95	1.78	3	2835.63	CrII(005)	1.54	P	30	double peaked
					2835.716	FeII(216)	3.18	S		
2836.56		66		1				P		U
2837.61	0.70	58	0.91	2	2837.300	FeII(231)	3.25	P	33	
2838.41		48		1	2838.120	Fe I(044)	0.99	P	31	
2839.26		45		1				P		U
2840.21		82		1	2840.01	CrII(082)	3.73	P	21	
2840.81	1.71	95	B B	1	2840.342	FeII(195)	3.14	P	49	too strong
					2841.354	FeII(196)	3.19	S		
2842.16	1.05	78	1.65	2	2841.914	TiII(007)	0.60	P	26	
					2842.076	FeII(196)	3.21	M		
					2843.24	CrII(005)	1.52	M		
					2843.323	FeII(231)	3.25	S		
2843.61	0.90	98	1.59	2	2843.485	FeII(294)	3.87	P	13	
					2843.631	Fe I(043)	0.91	M		
2845.71	0.45	49	1.17	1				P		U
2847.96	0.86	82	1.13	1*	2848.046	FeII(196)	3.22	P	-8	
					2848.15	CrII(081)	3.72	S		
					2849.33	CrII(081)	3.74	M		
					2849.601	FeII(196)	3.19	M		
2849.91	1.38	97	0.92	3	2849.83	CrII(005)	1.50	P	8	
					2851.798	Fe I(044)	1.01	M		
2852.11	1.32	100	0.57	3	2852.120	Mg I(001)	0.00	P	0	variable, wind
					2852.864	FeII(219)	3.32	M		
					2853.18	CrII(081)	3.73	S		
2853.16	0.72	60	1.29	1*	2853.199	FeII(197)	3.22	P	-3	
2855.91	1.32	97	1.78	3	2855.67	CrII(005)	1.49	P	25	
					2855.676	FeII(196)	3.21	M		
2857.36		85		2	2857.171	FeII(294)	3.87	P	20	
2858.96	1.56	95	0.74	2	2858.91	CrII(005)	1.54	P	5	
2861.16	1.20	92	1.20	3	2860.92	CrII(005)	1.48	P	25	
					2861.187	FeII(061)	1.07	M		
2862.71	0.96	95	1.23	3	2862.57	CrII(005)	1.52	P	15	
2864.41		58		1	2864.367	FeII(195)	3.22	P	5	
2865.36	1.56	94	1.52	2	2865.10	CrII(005)	1.50	P	27	double peaked
					2865.34	CrII(011)	2.41	S		
2867.02	1.30	90	R B	1	2866.72	CrII(005)	1.49	P	31	
					2867.09	CrII(011)	2.42	M		
					2867.09	CrII(011)	2.42	M		
2867.72	1.32	90	B B	1	2867.65	CrII(005)	1.48	P	7	
					2868.63	CrII(057)	3.74	M		
					2868.732	TiII(005)	0.57	M		
2869.07	1.30	94	1.23	2	2868.874	FeII(061)	1.04	P	20	
2870.72	1.60	89	1.13	1	2870.43	CrII(011)	2.44	P	30	variable
					2870.608	FeII(195)	3.21	S		
2871.52		69		1	2871.059	FeII(195)	3.19	P	48	
					2871.125	FeII(230)	3.23	S		line ?

Table 6. continued

λ_{obs} [Å]	W [Å]	D [%]	A	Q	λ_{lab} [Å]	ion(mult)	χ [eV]	C	v [km s ⁻¹]	remark
2872.31	0.70	74	1.14	3*	2872.382	FeII(230)	3.25	P	-7	
2873.92	1.40	92	0.88	1	2873.46	CrII(005)	1.49	P	48	
					2873.81	CrII(011)	2.42	M		
					2875.97	CrII(011)	2.47	M		
2876.32	1.90	97	1.55	2	2876.24	CrII(005)	1.50	P	8	
					2876.30	CrII(288)	4.96	M		
2879.72		73		1	2879.485	MnII(061)	4.09	P	24	
					2879.543	FeII(230)	3.23	S		
2880.12		77		1	2880.026	V II(012)	0.35	P	10	
2880.82	0.92	97	1.14	3	2880.750	FeII(061)	0.98	P	7	
2882.72	0.51	73	0.86	2	2882.493	V II(012)	0.33	P	24	too strong
2884.22	1.10	86	1.44	1	2886.234	FeII(229)	3.23	S		U
2886.82	1.14	74	1.08	1	2886.670	MnII(060)	4.11	P	16	
2888.07		60		1	2887.882	MnII(061)	4.10	P	20	
2888.47		68		1	2888.089	FeII(215)	3.18	P	40	
2888.32		90		1	2889.19	CrII(011)	2.47	M		
2889.57	1.54	94	0.86	1	2889.528	MnII(060)	4.10	P	4	
2889.57	1.54	94	0.86	1	2889.605	MnII(060)	4.09	P	-3	Wind?
					2891.050	TiII(005)	0.60	M		
					2891.333	MnII(069)	4.49	M		
2891.72	1.10	89	1.44	1	2891.636	V II(012)	0.33	P	9	
2892.46		97		1*	2892.434	V II(012)	0.37	P	3	
					2892.650	V II(012)	0.35	M		
2893.42		92		1	2893.314	V II(012)	0.37	P	11	
					2897.24	CrII(287)	4.96	M		
2897.57		77		1	2897.264	FeII(254)	3.41	P	32	
2898.82		71		3	2898.53	CrII(095)	3.85	P	30	
					2898.703	MnII(061)	4.11	M		
2900.21	0.36	52	1.20	3*	2900.154	MnII(069)	4.48	P	6	
2901.52	0.30	29	1.20	3				P		U
2904.42	0.38	40	1.14	1	2906.120	FeII(215)	3.32	S		
2906.62	0.79	84	0.84	2	2906.35	Mg I(004)	2.70	P	28	
					2906.448	V II(011)	0.35	M		
					2906.76	CrII(057)	3.81	M		
					2907.457	V II(010)	0.37	M		
2908.02	0.95	81	1.20	1	2907.853	FeII(060)	0.98	P	17	
2909.02	0.63	89	0.88	3	2908.810	V II(012)	0.39	P	22	
					2910.007	V II(011)	0.33	M		
2910.32	0.80	90		1	2910.380	V II(011)	0.32	P	-5	
2911.17	0.33	55	1.00	1	2911.050	V II(010)	0.35	P	12	
2912.07	0.39	55	1.17	3	2912.158	Fe I(001)	0.00	P	-8	possible IS
2916.37	0.85	71	0.67	1	2916.150	FeII(060)	0.98	P	23	
					2916.933	FeII(229)	3.25	M		

Table 6. continued

λ_{obs} [Å]	W [Å]	D [%]	A	Q	λ_{lab} [Å]	ion(mult)	χ [eV]	C	v [km s ⁻¹]	remark	
					2917.087	FeII(336)	4.48	M			
					2917.365	V II(011)	0.33	M			
2917.62	0.75	87	1.07	3	2917.465	FeII(061)	1.04	P	16		
					2919.989	V II(011)	0.37	M			
					2920.377	V II(011)	0.35	S			
2920.47	0.74	84	1.64	1	2920.377	V II(010)	0.33	P	10		
2921.41		66		1*	2921.23	CrII(286)	4.96	P	18		
2922.12	0.70	68	B B	1	2921.81	CrII(095)	3.85	P	32		
2924.12		97		3	2924.017	V II(010)	0.39	P	11		
2924.62		84		1	2924.633	V II(010)	0.37	P	0		
					2926.15	CrII(095)	3.85	M			
2926.77	1.02	95	1.57	3	2926.584	FeII(060)	0.98	P	19		
2928.41		81		1*	2928.32	CrII(095)	3.84	P	9		
2928.61		84		1*	2928.625	MgII(002)	4.40	P	-1		
2930.97	0.75	76	1.13	3	2930.798	V II(010)	0.35	P	18		
					2930.83	CrII(055)	3.70	M			
					2932.69	CrII(095)	3.85	M			
2933.22	1.05	97	1.00	2	2933.051	MnII(005)	1.17	P	17		
					2933.466	FeII(307)	3.95	M			
2935.27	0.90	76	B B	3	2935.12	CrII(055)	3.81	P	15		
2936.92	1.18	94		1.10	1	2936.469	Mg I(003)	2.70	P	46	
					2936.496	MgII(002)	4.41	S			
					2936.735	Mg I(003)	2.70	M			
2939.52	1.21	97	1.16	2	2939.302	MnII(005)	1.17	P	22		
2939.52	1.21	97	1.16	2	2939.506	FeII(060)	1.04	P	1		
					2941.32	CrII(095)	3.85	M			
					2941.343	Fe I(001)	0.09	M			
2941.62	1.20	90	1.75	1	2941.372	V II(010)	0.39	P	25		
					2941.485	V II(010)	0.33	M			
2944.67	1.38	95	1.53	1	2944.399	FeII(078)	1.69	P	28		
					2944.568	V II(010)	0.37	M			
2946.37	0.01	6	1.00	2	2946.173	FeII(307)	3.95	P	20		
2947.82	1.21	95	0.82	3	2947.658	FeII(078)	1.66	P	16		
					2947.877	Fe I(001)	0.05	M			
2949.42	1.04	98	1.27	3	2949.201	MnII(005)	1.17	P	22		
2950.47	0.56	71	2.33	2	2950.344	V II(010)	0.32	P	13		
					2951.871	MnII(068)	4.49	M			
2952.22	0.53	79	1.29	2	2952.07	V II(010)	0.35	P	15		
					2953.34	CrII(055)	3.70	M			
2953.94	1.27	97	1.56	3	2953.774	FeII(060)	1.04	P	17		
					2953.940	Fe I(001)	0.09	M			
					2954.050	FeII(253)	3.37	M			
2957.67	0.72	84	1.29	3	2957.365	Fe I(001)	0.11	P	31		
					2957.520	V II(010)	0.33	M			
2959.82	0.82	74	1.15	2	2959.601	FeII(254)	3.37	P	22		
2961.52	0.65	82	1.43	2	2961.272	FeII(060)	1.07	P	25		
2964.72	1.07	89	R B	1	2964.629	FeII(078)	1.72	P	9		
					2965.036	FeII(078)	1.69	S			

Table 6. continued

λ_{obs} [Å]	W [Å]	D [%]	A	Q	λ_{lab} [Å]	ion(mult)	χ [eV]	C	v [km s ⁻¹]	remark
2965.12		94		1	2965.036	FeII(078)	1.69	P	8	
2966.37		68		3				P		U
2967.02	0.76	84	0.89	3	2966.901	Fe I(001)	0.00	P	12	
2968.57	0.56	81	R B	3				P		U
2969.12		56		1	2968.738	FeII(253)	3.37	P	39	
					2970.106	Fe I(001)	0.11	M		
2970.47	1.58	95	0.89	1	2970.510	FeII(060)	1.07	P	-3	
2972.12	1.00	90	1.44	3	2971.90	CrII(080)	3.75	P	22	
2973.32	0.85	76	1.10	2	2973.134	Fe I(001)	0.09	P	19	
2973.32	0.85	76	1.10	2	2973.237	Fe I(001)	0.05	P	8	
2976.17	1.10	87	R B	1	2975.938	FeII(060)	1.09	P	23	
2979.67	1.32	89	1.10	2	2979.349	FeII(060)	1.09	P	32	
2981.02		37		1	2980.963	FeII(253)	3.41	P	6	
2982.05	0.88	73		3*	2982.059	FeII(335)	4.46	P	0	
2983.67	0.34	74	1.25	1				P		U; NiII(66) in Sun; not in α Lep
					2984.69	CrII(055)	3.74	M		
2984.97	0.84	98	R B	1	2984.831	FeII(078)	1.66	P	14	
					2985.32	CrII(080)	3.73	M		
					2985.32	CrII(080)	3.73	M		
2985.62	1.08	97	B B	1	2985.545	FeII(078)	1.72	P	8	
2986.92	0.30	48	1.00	3	2986.617	FeII(254)	3.41	P	30	
2988.42	0.10	24	1.17	2	2988.04	CrII(080)	3.75	P	38	
2989.52	0.70	69	1.29	2	2989.18	CrII(080)	3.72	P	34	
2992.82	0.34	48	1.17	3	2992.42	CrII(080)	3.74	P	40	
2993.10		29		1*	2993.366	FeII(335)	4.48	P	-26	
2994.92		63		1	2994.74	CrII(080)	3.73	P	18	
2997.62	0.42	56	1.33	3	2997.298	FeII(335)	4.48	P	32	